Paracetamol analogues conjugated by FAAH induce TRPV1-mediated antinociception without causing acute liver toxicity

Johan Å.Nilsson, Christophe Mallet, Kiseko Shionoya, Anders Blomgren, Anders Sundin, Lars Grundemar, Ludivine Boudieu, Anders Blomqvist, Alain Eschalier, Ulf Nilsson, et al.

European Journal of Medicinal Chemistry 213 (2021) 113042

Contents lists available at ScienceDirect

European Journal of Medicinal Chemistry

journal homepage: http://www.elsevier.com/locate/ejmech

Research paper

Paracetamol analogues conjugated by FAAH induce TRPV1-mediated antinociception without causing acute liver toxicity

Johan L. Å.Nilsson [a], Christophe Mallet [b, c], Kiseko Shionoya [d], Anders Blomgren [a], Anders P. Sundin [e], Lars Grundemar [a], Ludivine Boudieu [b, c], Anders Blomqvist [d], Alain Eschalier [b, c], Ulf J. Nilsson [e], Peter M. Zygmunt [f, *]

[a] Division of Clinical Chemistry and Pharmacology, Department of Laboratory Medicine, Lund University, Box 117, SE-221 00, Lund, Sweden
[b] Université Clermont Auvergne, INSERM, NEURO-DOL Basics & Clinical Pharmacology of Pain, F-63000, Clermont-Ferrand, France
[c] ANALGESIA Institute, Faculty of Medicine, F-63000, Clermont-Ferrand, France
[d] Division of Neurobiology, Department of Biomedical and Clinical Sciences, Linköping University, SE-581 85, Linköping, Sweden
[e] Centre for Analysis and Synthesis, Department of Chemistry, Lund University, 221 00, Lund, Sweden
[f] Department of Clinical Sciences Malmö, Lund University, SE-214 28, Malmö, Sweden

ARTICLE INFO

Article history:
Received 17 September 2020
Received in revised form
3 November 2020
Accepted 16 November 2020
Available online 21 November 2020

Keywords:
Paracetamol
Acetaminophen
TRP channel
TRPV1
FAAH
Analgesic
Pain
Fever

ABSTRACT

Paracetamol, one of the most widely used pain-relieving drugs, is deacetylated to 4-aminophenol (4-AP) that undergoes fatty acid amide hydrolase (FAAH)-dependent biotransformation into *N*-arachidonoylphenolamine (AM404), which mediates TRPV1-dependent antinociception in the brain of rodents. However, paracetamol is also converted to the liver-toxic metabolite *N*-acetyl-*p*-benzoquinone imine already at therapeutic doses, urging for safer paracetamol analogues. Primary amine analogues with chemical structures similar to paracetamol were evaluated for their propensity to undergo FAAH-dependent *N*-arachidonoyl conjugation into TRPV1 activators both *in vitro* and *in vivo* in rodents. The antinociceptive and antipyretic activity of paracetamol and primary amine analogues was examined with regard to FAAH and TRPV1 as well as if these analogues produced acute liver toxicity. 5-Amino-2-methoxyphenol (**2**) and 5-aminoindazole (**3**) displayed efficient target protein interactions with a dose-dependent antinociceptive effect in the mice formalin test, which in the second phase was dependent on FAAH and TRPV1. No hepatotoxicity of the FAAH substrates transformed into TRPV1 activators was observed. While paracetamol attenuates pyrexia via inhibition of brain cyclooxygenase, its antinociceptive FAAH substrate 4-AP was not antipyretic, suggesting separate mechanisms for the antipyretic and antinociceptive effect of paracetamol. Furthermore, compound **3** reduced fever without a brain cyclooxygenase inhibitory action. The data support our view that analgesics and antipyretics without liver toxicity can be derived from paracetamol. Thus, research into the molecular actions of paracetamol could pave the way for the discovery of analgesics and antipyretics with a better benefit-to-risk ratio.

1. Introduction

The pharmacological options for analgesic therapy are limited with only a few distinct drug classes on the market. For many chronic pain conditions the analgesic treatments do not offer adequate pain relief and are often associated with adverse effects that limit a long-term use. Today, this is highlighted by the opioid crisis urging for the discovery of new analgesics. Paracetamol (acetaminophen) is one of the most used fever and pain-relieving drugs worldwide and its consumption increases [1,2]. It is currently recommended as first-line pharmacological therapy for many pain conditions, although some observations show that paracetamol has a limited efficacy, particularly in several chronic painful conditions including osteoarthritis [3–6] and low back pain [3,7]. Variation in human genotype may also contribute to the variable effectiveness of paracetamol as an analgesic [8]. Furthermore, paracetamol is converted into the liver-toxic metabolite *N*-acetyl-*p*-benzoquinone imine (NAPQI) already at therapeutic doses,

* Corresponding author.
E-mail address: peter.zygmunt@med.lu.se (P.M. Zygmunt).

https://doi.org/10.1016/j.ejmech.2020.113042

Abbreviations

4-AP	4-aminophenol
ALT	alanine aminotransferase
AM404	*N*-arachidonoylphenolamine
AST	aspartate aminotransferase
COX	cyclooxygenase
FAAH	fatty acid amide hydrolase
HMBA	4-(aminomethyl-2-methoxyphenol)
LPS	lipopolysaccharide
NAPQI	*N*-acetyl-*p*-benzoquinone imine
PG	prostaglandin
TRP	transient receptor potential
TRPV1	transient receptor potential vanilloid 1
TX	thromboxane

causing hepatotoxicity, a well-known adverse effect of the drug [9–11] making paracetamol the principal cause of acute liver failure in the Western world [12–15].

In a series of publications, we have developed a conceptual framework for the antinociceptive action of paracetamol, involving fatty acid amide hydrolase (FAAH) and TRPV1 [16–20]. Accordingly, paracetamol as a prodrug undergoes hepatic deacetylation into 4-aminophenol (4-AP) followed by conjugation of 4-AP with arachidonic acid through a FAAH-dependent mechanism in the brain yielding *N*-arachidonoylphenolamine (AM404). While the endogenous role of FAAH mainly is to hydrolyse anandamide and related *N*-acylethanolamines [21], it can also synthesize *N*-arachidonoyl conjugates, including AM404 and arvanil [16–18]. Activation of TRPV1 in the brain by AM404 and arvanil induces antinociception, and previous reports have demonstrated that modulation of supraspinal FAAH and TRPV1 activity affects nociceptive signaling as well as that FAAH and TRPV1 are critical for the antinociceptive efficacy of paracetamol in mice [17–20,22–26]. It has also been shown that AM404 inhibits cyclooxygenase (COX)-2 [16,27], which could explain the antipyretic effect of paracetamol. Noteworthy, AM404 has not only been identified in the brain of rodents, but also in human cerebrospinal fluid after paracetamol administration [28]. Furthermore, there is genetic evidence that TRPV1 is involved in the analgesic action of paracetamol in humans [8].

The objective of this study was to understand the structure-activity relationship of paracetamol and primary amine analogues that undergo a FAAH-dependent biotransformation into *N*-arachidonoyl conjugates (Fig. 1) mediating a TRPV1-induced antinociception, and to examine if these analogues could produce antinociception without causing acute liver toxicity. The antipyretic effect of paracetamol and analogues was also examined.

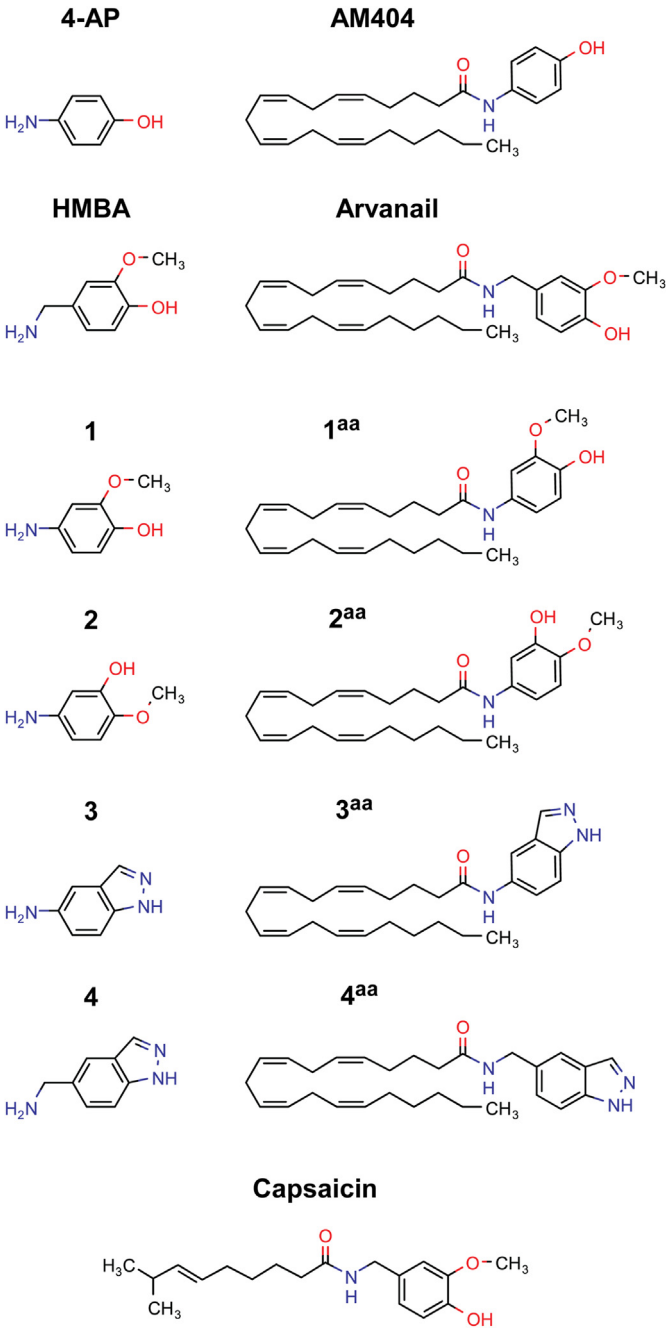

Fig. 1. The chemical structures of the primary amines 4-aminophenol (**4-AP**), 4-(aminomethyl)-2-methoxyphenol (**HMBA**), 4-amino-2-methoxyphenol (**1**), 5-amino-2-methoxyphenol (**2**), 5-aminoindazole (**3**), 5-aminomethyl indazole (**4**) and their corresponding *N*-arachidonoyl conjugates. Shown is also the structure of the prototypic TRPV1 activator capsaicin.

2. Methods

2.1. Drugs

4-Aminophenol, 4-(aminomethyl)-2-methoxyphenol (HMBA), 4-amino-2-methoxyphenol (**1**), 5-amino-2-methoxyphenol (**2**), 5-aminoindazole (**3**), 5-aminomethyl indazole (**4**), paracetamol, capsazepine, ibuprofen and Nω-nitro-L-arginine and phenylephrine were purchased from Sigma-Aldrich (St Louis, MO, USA). Indomethacin (Confortide®) was obtained from Dumex (Copenhagen, Denmark). *N*-arachidonoyl conjugates: *N*-(4-hydroxyphenyl)-5Z,8Z,11Z,14Z-eicosatetraenamide (AM404), *N*-(4-hydroxyphenyl)-5Z,8Z,11Z,14Z-eicosatetraenamide-d4 (AM404-d4), *N*-(4-hydroxy-3-methoxybenzyl)-5Z,8Z,11Z,14Z-eicosatetraenamide (arvanil), methyl arachidonyl fluorophosphonate (MAFP) and 3′-carbamoyl-6-hydroxy-[1,1′-biphenyl]-3-ylcyclohexylcarbamate (URB937) were purchased from Cayman Chemicals (Ann Arbor, MI, USA). *N*-(4-hydroxy-3-methoxyphenyl)-5Z,8Z,11Z,14Z-eicosatetraenamide (**1aa**; conjugate of 4-amino-2-methoxyphenol) and *N*-(3-hydroxy-4-methoxyphenyl)-5Z,8Z,11Z,14Z-eicosatetraenamide (**2aa**; conjugate of 5-amino-2-methoxyphenol) were purchased from Bioduro (San Diego, CA, USA). *N*-(1H-indazol-5-yl) 5Z,8Z,11Z,14Z-eicosatetraenamide (**3aa**; conjugate of 5-aminoindazole) and *N*-(1H-

indazol-5-ylmethyl) 5Z,8Z,11Z,14Z-eicosatetraenamide (**4**^{aa}; conjugate of 5-aminomethyl indazole) were synthesised by Red Glead Discovery AB (Lund, Sweden). All *N*-arachidonoyl conjugates were dissolved in ethanol. Primary amines were dissolved in physiological saline, occasionally supplemented with 5% DMSO. Intraperitoneal injections were given in volumes of 5–20 ml kg^{-1}. Capsazepine and URB937 were dissolved in DMSO/saline (1:9) for *in vivo* use. Drug solutions were prepared immediately before use.

2.2. Computational studies

All molecular modelling was performed using the Schrödinger 2018 software suite (Schrödinger Release 2017-3, Schrödinger, LLC, New York, NY, 2017). The model of FAAH was constructed based on electron diffraction data (X-ray, PDB: 3PR0, 2.2 Å), whereas the model of TRPV1 was constructed from a cryo-EM structure (PDB: 5IRZ, 3.28 Å) [29,30]. Protein structures for docking simulations were prepared using Maestro's Protein Preparation Wizard. The corresponding *N*-arachidonoyl conjugates of 4-AP (i.e. AM404), and of the paracetamol analogues 5-amino-2-methoxyphenol (compound **2**) and 5-aminoindazole (compound **3**) were manually placed in the capsaicin-binding pocket of TRPV1, and FAAH models of bound *N*-arachidonoyl conjugates were constructed by superimposing each conjugate with anandamide covalently bound to FAAH. These procedures were followed by an energy minimization with the OPLS-3 force field and the GB/SA solvation method for water.

2.3. Animals

All experiments were approved by the Linköping and Lund Animal Ethic Committees (ethical permission No. 44/13 (ID1854), M 48–13, M 49–134818/2017, 44-13; ID 1854) as well as the local French ethical committees (CEMEA Auvergne, France, ethical permission No. 02175.02). Experiments were performed according to European legislation (Directive 2010/63/EU) on the protection of animals used for scientific purposes, and complied with the recommendations of the International Association for the Study of Pain [31]. The design, analysis and reporting of the research complied with the ARRIVE guidelines [32]. All efforts were made to minimize discomfort and use as few animals as possible. Male Wistar rats (200–250 g) were purchased from Charles River Laboratories (RRID:RGD_10395233, Sulzfeld, Germany). FAAH$^{-/-}$ and FAAH$^{+/+}$ mice, originally generated by Benjamin Cravatt [33] and back-crossed with C57BL/6 mice for at least ten generations in our laboratory, were obtained from our own homozygous breeding for 2–3 generations. To minimize the number of animals used for the *in vitro* and *in vivo* FAAH metabolic studies, both male (25–35 g) and female (18–25 g) mice were used as previous studies have not revealed any difference between sex with regard to such studies [16–18]. For behavioural and temperature recording studies, eight-week-old male C57BL/6 mice were obtained from Janvier Laboratories and (RRID:MGI:5657942, Le Genest-Saint-Isle, France). All mice were kept 4–6 *per* cage at specific pathogen free facilities and fed *ad libitum* under controlled conditions with a 12 h light-dark cycle. At the end of the experiment animals were euthanized by CO_2 inhalation. For liver toxicity studies, eight-week old male C57BL/6 mice were obtained from Charles River Laboratories (RRID:RGD_10395233, Sulzfeld, Germany).

2.4. TRPV1-mediated vasorelaxation

The TRPV1 potency of *N*-arachidonoyl conjugates was assessed using mesenteric arteries from rats by recording the nerve-mediated vasorelaxation [16,18,34]. In short, arterial segments were dissected and mounted in organ baths between two force sensitive wires at a tension corresponding to a blood pressure of 90 mm Hg. The surrounding buffer was composed of a physiological salt solution (NaCl 119, KCl 4.6, $CaCl_2$ 1.5, $MgCl_2$ 1.2, $NaHCO_3$ 15, NaH_2PO_4 1.2 and D-glucose 6 (mM); pH 7.4) which was temperature-controlled (37 °C) and aerated with 95% O_2 and 5% CO_2. To create an environment in which phenylephrine (dissolved in saline) induces stable and long-lasting contractions all experiments were performed in the presence of indomethacin (10 μM) and Nω-nitro-L-arginine (100 μM), both dissolved in saline, to diminish the production of COX- and nitric oxide synthase-derived vasodilators, respectively. After submaximal vasoconstriction mediated by phenylephrine (3 μM), the arteries were exposed to *N*-arachidonoyl conjugates (dissolved in ethanol) to estimate their sensory-nerve mediated vasodilator properties in the absence and presence of the TRPV1 antagonist capsazepine (3 μM) dissolved in ethanol. The final concentration of ethanol reached 1% and does not affect blood vessel contractile properties [16,18,34]. Changes in the tension of vessels were registered by the force-displacement transducer model FT03C (Grass Instruments; Rhode Island, USA).

2.5. Evaluation of FAAH-mediated conjugation in vitro

Brains from FAAH$^{-/-}$ and FAAH$^{+/+}$ mice were removed and frozen in liquid nitrogen and homogenized in 4 ml ice-cold 10 mM Tris buffer supplemented with 1 mM EDTA and 0.3 mM ascorbic acid. The homogenate was divided into aliquots of 200 μl and preheated to 37 °C prior to addition of primary amines (0.1 mM). The samples were incubated at 37 °C under stirring for 20 min before the reaction was stopped by adding 1 ml of ice-cold acetone containing an internal standard (AM404-d4). The conjugate content of samples was determined using the LC-MS/MS technique (see below). For details on methodology, see Refs. [16–18].

2.6. Evaluation of FAAH-mediated conjugation in vivo

FAAH$^{-/-}$ and FAAH$^{+/+}$ mice were injected intraperitoneally (i.p.) with the primary amines (100 or 300 ml kg^{-1}) dissolved in saline (occasionally supplemented with 5% DMSO). The animals were anesthetized with isoflurane and decapitated 20 min after the injection. The brains were removed and promptly frozen in liquid nitrogen, and stored at −80 °C. They were homogenized in 2 ml ice-cold 10 mM Tris buffer, which had been supplemented with 1 mM EDTA and 0.3 mM ascorbic acid and 10 μM of the FAAH inhibitor MAFP to prevent *N*-arachidonoyl formation and degradation *post mortem*. To determine *N*-arachidonoyl conjugate levels, aliquots of 200 μl homogenate were precipitated with 1 ml ice-cold acetone containing 0.3 mM ascorbic acid, 5 nM AM404-d4 (Cayman Chemicals) and 10 nM PGE_1-d4 (Cayman Chemicals), as internal standards, and analyzed by the LC-MS/MS technique (see below). For details on methodology, see Refs. [16–18].

2.7. Lipopolysaccharide-induced fever and prostanoid levels in vivo

Lipopolysaccharide (LPS), 100 μg kg^{-1} i.p. from *Escherichia coli* (O111:B4; Sigma-Aldrich, St. Louis, MO), or saline was administered 3 h prior to i.p. injection of paracetamol (100 and 150 mg kg^{-1}), 4-AP (30 mg kg^{-1}), **3** (25 mg kg^{-1}), or their vehicle [Ringer's acetate solution, Fresenius Kabi AB, Uppsala, Sweden (Na^+ 131 mM, Cl^- 112 mM, acetate 30 mM, K^+ 4 mM, Ca^{2+} 2 mM, Mg^{2+} 1 mM)]. Forty minutes after the injection, the animals were anesthetized with isoflurane and decapitated. Blood was collected from carotid arteries into heparin tubes containing sodium citrate and the COX-inhibitor ibuprofen. The brain was removed and the diencephalon, including the hypothalamus (considered to be the site of the

antipyretic effect of paracetamol through COX inhibition [35]) was promptly dissected, snap frozen in liquid nitrogen, and stored at −80 °C. The diencephalon was homogenized in 1 ml ice-cold 10 mM Tris buffer, to which had been added 1 mM EDTA, 300 μM ascorbic acid, 10 μM MAFP and 100 μM ibuprofen, the latter to prevent *in vitro* prostanoid formation and degradation. In order to determine prostanoid levels, aliquots (200 μl) of blood and homogenates of the diencephalon were precipitated with 1 ml ice-cold acetone, containing 300 μM ascorbic acid and 10 nM PGE_1-d4 (Cayman Chemicals, Co., Ann Arbor, USA) as internal standard, and analyzed by the LC-MS/MS technique (see below).

For details on telemetric temperature recordings, see Refs. [36,37]. In short, under anesthesia (1% isoflurane, Abbot Scandinavia, Solna, Sweden), a temperature-recording probe was implanted intraperitoneally (TA11TAF10; Data Sciences International, St. Paul, MN, USA) and postoperative analgesia was given with buprenorphine (Temgesic, 100 mg kg^{-1} in 0.1 ml saline i.p.; RB Pharmaceuticals, Slough, Berkshire, United Kingdom). To provide near-thermoneutral conditions the mice were transferred to a room in which the ambient temperature was set to 29 °C. The animals were let to recover for at least 1 week before start of experiments.

2.8. Quantitative LC-MS/MS analysis

All precipitated samples were centrifuged at 17960 g for 10 min at 4 °C. The supernatants were vacuum evaporated and each extraction residual was subsequently reconstituted in 200 μl of a mixture of 99.5% methanol and 0.5% acetic acid (for *N*-arachidonoyl conjugates) or 80% methanol, 19.5% H_2O and 0.5% acetic acid (for prostanoids). The protein content of the pellet was determined by Coomassie protein assay (Pierce, IL, USA), using bovine serum albumin as standard reference.

All samples were analyzed on a Shimadzu HPLC system (Shimadzu, Kyoto, Japan) coupled to a Sciex 5500 tandem mass spectrometer (Applied Biosystems/MDS Sciex, Darmstadt, Germany). Sample aliquots of 5 μl were injected onto a Waters CSH C_{18} column (50 × 2 mm, 3 μm (Waters, Milford, MA, USA)) held at 50 °C. All mobile phases were water-acetonitrile gradients, containing 0.1% formic acid and with a flow rate of 500 μl min^{-1}. The acetonitrile content was initially 20%, then increased linearly to 100% over 3 min and kept at this level for 3 min 15 s, followed by an equilibration at 20% for 45 s.

All *N*-arachidonoyl conjugates were quantified by LC-MS/MS with the electrospray interface operating in a positive ion mode at 550 °C with the ion spray voltage set to 5000 V. The prostanoids PGE_2 (Sigma-Aldrich, Schnelldorf, Germany), $PGF_{2\alpha}$ (Sigma-Aldrich), 6-keto-$PGF_{1\alpha}$ (Cayman Chemicals) and TXB_2 (Biomol GmbH, Hamburg, Germany) were quantified by LC-MS/MS with the electrospray interface operating in a negative ion mode at 550 °C with the ion spray voltage set to −4500 V. The mass transitions (*m*/*z*) for *N*-arachidonoyl conjugates and prostanoids were as follows: 396.2/110.0 (AM404); 400.2/287.4 (AM404-d4); 440.3/137.1 (arvanil); 426.3/140.1 (**1**^{aa} and **2**^{aa}); 420.3/134.1 (**3**^{aa}); 434.0/131.2 (**4**^{aa}); 351.2/315.3 (PGE_2); 357.2/321.2 (PGE_1-d4); 369.2/169.1 (TXB_2); 353.4/309.3 ($PGF_{2\alpha}$) and 369.4/163.1 (6-keto-$PGF_{1\alpha}$).

N-arachidonoyl conjugates and prostanoids were analyzed using AM404-d4 and PGE_1-d4, respectively, as internal standard. The detection limits were calculated as the concentrations corresponding to three times the standard deviation of the blanks. When levels were below detection limit for *N*-arachidonoyl conjugates (AM404, 3.58 pmol g^{-1} protein; arvanil, 14.34 pmolg^{-1} protein; **1**^{aa}, 14.34 pmolg^{-1} protein; **2**^{aa}, 3.58 pmolg^{-1} protein; **3**^{aa}, 3.58 pmolg^{-1} protein; **4**^{aa}, 14.34 pmol g^{-1} protein) and prostanoids (PGE_2, 493.26 pmol·g^{-1} protein; TXB_2, 162.88 pmol·g^{-1} protein; 6-keto-$PGF1_\alpha$, 264.30 pmol g^{-1} protein; $PGF_{2\alpha}$, 1874.68 pmol g^{-1} protein), numerical values of 1/4 of the detection limit were used in the calculations.

2.9. Animal behavioural tests

Animals were randomly divided into 5–10 per group. Randomized treatment administrations were performed according to the method of equal blocks to assess the effect of the different treatments at the same time interval to avoid unverifiable and time-variable environmental influences. All experiments were performed in a quiet room by the same blinded experimenter. To ensure the methodological quality of this study, we followed recommendations from Rice et al. [38]. The two compounds, **2** and **3**, were injected i.p., 10 min before locomotor or nociceptive tests. For intracerebroventricular (i.c.v.) administrations, URB937 was injected at a dose of 5 μg in 5 μl and capsazepine at a dose of 10 μg in 5 μl, 5 min before injection of compounds **2** or **3**.

Locomotor activity: Motor impairment was measured on a rotarod apparatus (Bioseb, Chaville, France). Before the test, animals were trained under continuous rotation (4 rpm) in 1-minute sessions. For the test, mice were placed individually on the revolving drum. Once mice were balanced, the drum was accelerated from 4 to 40 revolutions *per* minute over the course of 5 min. The time point at which each mouse fell off the rod was recorded.

Formalin test: The animals received an intraplantar injection of a 2.5% formalin solution (25 μl/mouse) into a hind paw. The time spent biting and licking of the injected paw was monitored during the two typical phases of the nociceptive response (phase I: 0–5 min; phase II: 15–40 min).

The i.c.v. administrations were performed following the method previously described [25]. In short, all animals were briefly anaesthetized with isoflurane (1–2%). The site of injection was 2 mm from either side of the median on a line drawn through the anterior base of the ears. Animals were injected with a volume of 5 μl using a 10 μl Hamilton syringe fitted with a 26-gauge needle with the tip adjusted to be inserted 2 mm deep.

2.10. Liver histology and aminotransferases activity

Mice were randomly allocated into one of the treatment groups. The food was withdrawn 12–16 h prior to the administration of substances. All substances were dissolved in saline (using minor heating) and administered at a dose of 300 mg kg^{-1} (i.p.), a dose often used to study paracetamol-induced liver injury in mice [39]. After 12 h the animals were briefly anesthetized with isoflurane and decapitated. The blood was collected in heparin tubes and the left medial hepatic lobe was removed for analysis.

Blood-containing heparin tubes were centrifuged at 2000 g for 10 min. The serum was collected and the aminotransferase activity was evaluated within 12 h using Cobas 6000/8000 analyzer series (Roche Diagnostics, Rotkreuz, Switzerland).

The excised liver tissue was fixed in 4% cold formaldehyde dissolved in PBS for 90 min and subsequently rinsed in PBS supplemented with 15% sucrose at 4 °C. Samples were then frozen in isopenthane before being cut serially at 10 μm, using a cryostat (Leica CM3050, Leica microsystems, Wetzlar, Germany). All sections were stained with haematoxylin & eosin (Sigma, St Louis, MO). A Nikon Eclipse TE2000-S bright-field microscope (Nikon, Tokyo, Japan) was used to evaluate the morphology.

2.11. Calculations and statistical analysis

GraphPad Prism 8 (GraphPad Software, La Jolla, CA) was used for statistical analysis and to perform curve fitting (non-linear

regressions) and calculations of pEC_{50} values (the negative log concentration that elicited half-maximal vasorelaxation). The level of statistical significance was set at $P < 0.05$. Comparisons between two groups of data were performed using Student's t-test. Comparisons of more than two groups of data were performed using 1-way ANOVA or repeated measures ANOVA followed by either Dunnett's, Tukey's or Sidak's multiple comparisons test, Welch's ANOVA test or 2-way ANOVA followed by Sidak's multiple comparisons test. Data are presented as the mean ± SEM; *n* indicates the number of animals examined.

3. Results

3.1. In vitro FAAH-mediated fatty acid conjugation of primary amines and evaluation of TRPV1 agonistic properties of the corresponding N-arachidonoyl conjugates

The paracetamol metabolite 4-AP as well as the primary amine 4-(aminomethyl)-2-methoxyphenol (HMBA) undergo FAAH-mediated fatty acid conjugation into the *N*-arachidonoyl conjugate AM404 and arvanil, respectively, both of which activate TRPV1 *in vitro* (Fig. 2, Table 1) [16–18]. Here, we have explored additional primary amino analogues in a LC-MS/MS based assay for evaluation of their predisposition to undergo FAAH-mediated fatty acid conjugation *in vitro* into their corresponding *N*-arachidonoyl conjugates denoted with ^{aa} (Fig. 2A, Table 1). The vanilloid structure 4-amino-2-methoxyphenol (**1**) was found to be a poor FAAH substrate, whereas the regioisomer 5-amino-2-methoxyphenol (**2**) was conjugated by FAAH in greater amounts, albeit less efficiently than 4-AP (Fig. 2A, Table 1). 5-Aminoindazole (**3**), a bioisostere of 4-AP, underwent a more efficient FAAH-mediated conjugation than 4-AP and 5-aminomethyl indazole (**4**) (Fig. 2A, Table 1). The aliphatic amines (**4**) and HMBA yielded similar amounts of their corresponding *N*-arachidonoyl conjugates, but less than the amount of AM404 produced by 4-AP (Fig. 2A, Table 1). The FAAH-dependent structural requirements of the conjugation of the primary amines was apparent by the reduced formation of their corresponding conjugates in $FAAH^{-/-}$ preparations (Table 1).

The TRPV1 agonistic properties of the *N*-arachidonoyl conjugates of compounds **1**–**4** were determined by their ability to induce a TRPV1-dependent primary sensory nerve-mediated vasorelaxation of pre-contracted rat isolated mesenteric arterial segments, an *in vitro* assay that has been extensively used in pharmacological studies of native TRPV1 [40]. In this assay, all *N*-arachidonoyl conjugates produced complete relaxations and were more potent than the TRPV1 active paracetamol metabolite AM404 (Fig. 2B, Table 2). The TRPV1 antagonist capsazepine significantly reduced the potency of each *N*-arachidonoyl conjugate similar to what has been shown previously for the TRPV1 agonists capsaicin, AM404 and arvanil [16,18,34] (Table 2).

Table 1
In vitro fatty acid conjugation of primary amines by FAAH into *N*-arachidonoyl conjugates.

Compound	*N*-arachidonoyl conjugates (nmol g^{-1} protein)			
	$FAAH^{+/+}$	*n*	$FAAH^{-/-}$	*n*
4-AP	8.8 ± 0.7	5	0.05 ± 0.02	3
HMBA	2.5 ± 0.3	7	0.01 ± 0.00	4
1	0.54 ± 0.09	6	0.005 ± 0.001	3
2	3.0 ± 0.1	6	0.06 ± 0.01	3
3	12 ± 0.6	6	0.09 ± 0.01	3
4	2.5 ± 0.2	5	0.04 ± 0.01	3

The fatty acid amide hydrolase (FAAH) *in vitro* activity was determined by measuring the content of *N*-arachidonoyl conjugates after incubation of brain homogenates from $FAAH^{+/+}$ or $FAAH^{-/-}$ mice with 0.1 mM of primary amines (Compound). Compared to AM404, the content of each other *N*-arachidonoyl conjugate was different in $FAAH^{+/+}$ mice (see also Fig. 2A) . Data are presented as mean ± SEM, and *n* denotes the number of animals.

3.2. In silico studies of the FAAH-mediated production of N-arachidonoyl conjugates and their interactions with TRPV1

To understand the interaction of the *N*-arachidonoyl conjugates with both target proteins, FAAH and TRPV1, the corresponding *N*-arachidonoyl conjugates of 4-AP, **2** and **3** were chosen as key compounds from the *in vitro* studies for modelling with FAAH (PDB: 3PR0, 2.2 Å, X-ray) and TRPV1 (PDB: 5IRZ, 3.28 Å, cryo-EM) [29,30]. The two proteins were prepared using the Protein Preparation Wizard Script within Maestro (Schrödinger Inc.) before manual introduction of the *N*-arachidonoyl conjugates of 4-AP, **2** and **3**.

The interaction of AM404 with FAAH was first studied (Fig. 3A). Upon FAAH-mediated conjugation of 4-AP, the tetrahedral intermediate of AM404 is covalently attached to Ser241 via its carbonyl carbon [41], whereas the amide hydrogen and nitrogen of AM404 are interacting with backbone Met191 and the hydroxyl group of

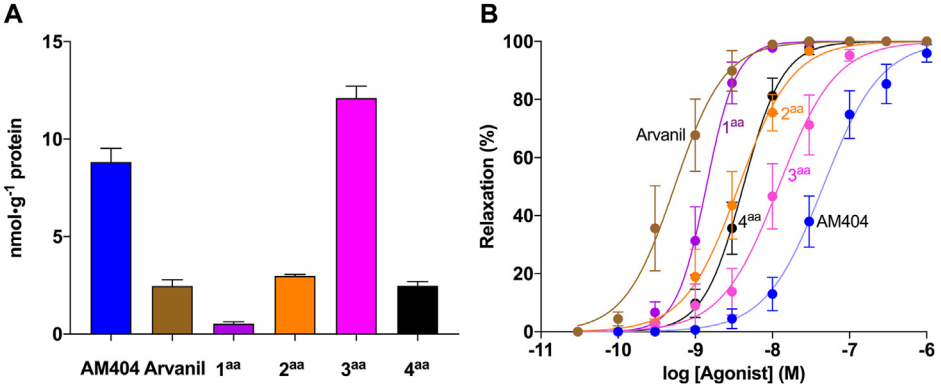

Fig. 2. *In vitro* fatty acid conjugation of primary amines by FAAH into corresponding *N*-arachidonoyl conjugates activating TRPV1. (**A**) *In vitro* FAAH activity was evaluated by the content of *N*-arachidonoyl conjugates after addition of primary amines (0.1 mM) to brain homogenate from $FAAH^{+/+}$ mice. The production of all *N*-arachidonoyl conjugates were FAAH-dependent (Table 1). Compared to AM404, the content of each other *N*-arachidonoyl conjugate was different in $FAAH^{+/+}$ mice ($P < 0.0001$, 1-way ANOVA followed by Sidak's multiple comparisons test, n=5-7). Also, using the same test, differences were observed between the *N*-arachidonoyl conjugates of the phenolic regioisomers **1** and **2** ($P < 0.0001$), and the indazoles **3** and **4** ($P < 0.0001$) ($n = 5–6$). (**B**) Concentration-response curves for TRPV1-mediated vasorelaxation of rat isolated mesenteric arteries evoked by the *N*-arachidonoyl conjugates ($n = 6–10$). The potency (pEC_{50}) of *N*-arachidonoyl conjugates are listed in Table 2. The TRPV1 antagonist capsazepine (3 μM) caused a rightward shift of the concentration-response curves without affecting the maximum relaxation (Table 2). Data are presented as mean ± SEM.

Table 2
TRPV1 potency of *N*-arachidonoyl conjugates

Compound	TRPV1 potency (pEC_{50})			
	Control	*n*	CZ	*n*
AM404	7.3 ± 0.1	10	n.d.	-
Arvanil	9.3 ± 0.2	6	n.d.	-
1^{aa}	8.9 ± 0.1	7	7.8 ± 0.2	6
2^{aa}	8.5 ± 0.1	8	7.2 ± 0.2	7
3^{aa}	7.9 ± 0.2	8	6.4 ± 0.4	6
4^{aa}	8.4 ± 0.1	8	6.8 ± 0.2	5

	AM404	Arvanil	**1**^{aa}	**2**^{aa}	**3**^{aa}	**4**^{aa}
AM404		****	****	****	*	****
Arvanil	****		ns	*	****	***
1^{aa}	****	ns		ns	**	ns
2^{aa}	****	*	ns		ns	ns
3^{aa}	*	****	**	ns		ns
4^{aa}	****	***	ns	ns	ns	

N-arachidonoyl conjugates of primary amines (Compound) were assessed for their ability to induce TRPV1-mediated relaxation of rat isolated mesenteric arteries. The negative log molar concentration of the conjugate that evoked half-maximal response (pEC_{50}) was calculated in the absence and presence of the TRPV1 antagonist capsazepine (CZ, 3 μM). Capsazepine significantly reduced the potency of each *N*-arachidonoyl conjugate ($P < 0.001$ for **1**, $P < 0.0001$ for **2**, $P < 0.01$ for **3** and $P < 0.0001$ for **4** using the Student's unpaired *t*-test). The potencies of *N*-arachidonoyl conjugates were compared by 1-way ANOVA followed by Tukey's multiple comparisons test (****$P < 0.0001$, ***$P < 0.001$, **$P < 0.01$, *$P < 0.05$; $P > 0.05$ is not significant = ns). Data are presented as mean ± SEM, and *n* denotes the number of animals. n.d. = not determined.

Ser217, respectively (Fig. 3A and B). Interestingly, two energy minima were observed, as the amide nitrogen of the covalently bound AM404 intermediate could assume either a pyramidal (sp3) or a planar (sp2) geometry. Similar to AM404, the *N*-arachidonoyl conjugates of **2** and **3** are displaying planar sp2 and pyramidal sp3 geometries, respectively, in their energy minima when bound to FAAH (Fig. 3C and D). Compared to 4-AP and **2**, the *N*-arachidonoyl conjugate of **3** assumes a planar amide nitrogen geometry at a lower energy state (**3**^{aa}: $\Delta E_{pyramidal\text{-}planar} = 14.4$ kJ mol^{-1} versus AM404: $\Delta E_{pyramidal\text{-}planar} = -3.1$ kJ mol^{-1} and **2**^{aa}: $\Delta E_{pyramidal\text{-}planar} = -23.2$ kJ mol^{-1}).

Next, the interaction of AM404 with TRPV1 was studied (Fig. 4). In TRPV1, AM404 was introduced to the capsaicin-binding site (Fig. 4A). The arachidonic tail of AM404 facilitates non-specific, hydrophobic interactions, similar to the hydrophobic moieties of the ultrapotent TRPV1 activator resiniferatoxin [42]. Furthermore, two polar interactions fixate the amide linker region of AM404 towards Tyr511 and Thr550 entrapping AM404 in a VR_{down} binding pose [30,43]. This geometry also allows for π-π interactions towards Tyr511. Additional polar interactions are formed between the hydroxyl group and Arg557/Glu570 in the TRPV1 S4–S5 linker region. *In vitro* data and insights from the computational studies regarding AM404 encouraged studies of the *N*-arachidonoyl conjugate of **3**, having an indazole moiety instead of a phenolic/vanilloid moiety as in AM404 and **2** (Fig. 4B). The conjugate with **3** assumed a binding mode within TRPV1 similar to AM404, only lacking an apparent π-π interaction towards Tyr511, but with closer contact to Arg557 and Glu570 through hydrogen accepting and donating atoms, respectively.

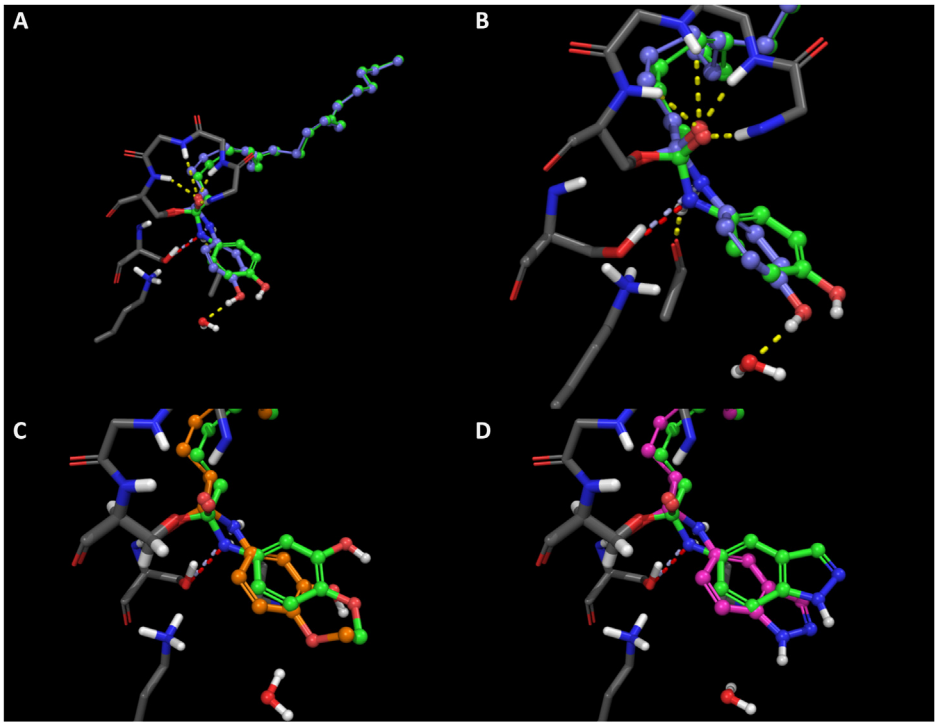

Fig. 3. Representative docking poses for the paracetamol metabolite AM404, **2** and **3** within FAAH. (**A**) FAAH is a ubiquitous, dimeric, membrane bound enzyme characterized by a distinctive catalytic triad (Ser241, Ser217, Lys142) and an oxyanion hole which stabilizes the carboxylic oxygen in the tetrahedral transition state of AM404, a geometry in the FAAH-mediated conjugation process that has been proposed as a stable intermediate [41,56]. (**B**) A planar (blue) and a pyramidal (green) geometry of the amide nitrogen of AM404 were observed ($\Delta E_{pyramidal\text{-}planar} = -3.1$ kJ mol^{-1}), which have different bond lengths towards Ser217 (red and light blue dots). (**C**,**D**) Like AM404 the *N*-arachidonoyl conjugates of **2** (**C**) and **3** (**D**) display planar (**2**, orange; **3**, magenta) and pyramidal (**2** and **3**, green) energy minima within FAAH ($\Delta E_{pyramidal\text{-}planar} = -23.2$ kJ mol^{-1}, and $\Delta E_{pyramidal\text{-}planar} = 14.4$ kJ mol^{-1}, respectively). Yellow dots show polar bonds. Only polar hydrogens are shown for clarity. (For interpretation of the references to colour in this figure legend, the reader is referred to the Web version of this article.)

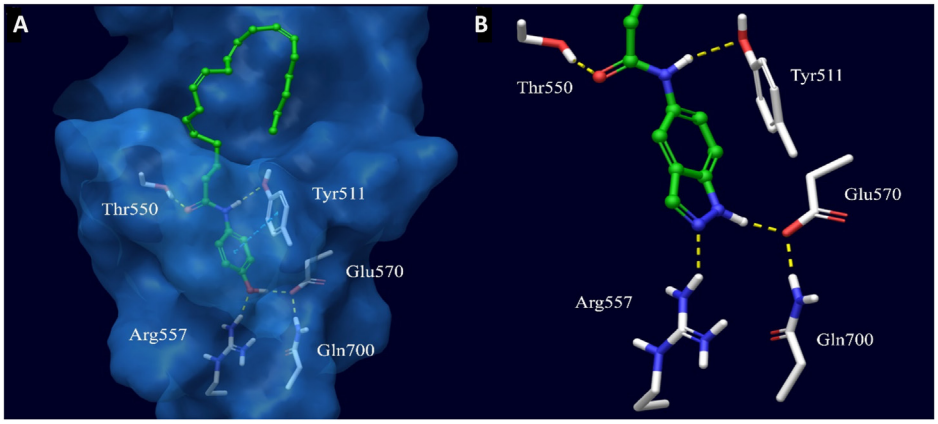

Fig. 4. Representative docking poses for the paracetamol metabolite AM404 and **3** within TRPV1. (**A**) AM404 binds to the capsaicin-binding pocket of TRPV1. The hydroxyl group of AM404 forms key interactions towards Glu570 and Arg557. (**B**) These interaction modes can be optimized, as exemplified by the *N*-arachidonoyl-conjugate of 5-aminoindazole (compound **3**). Polar bonds are represented as yellow dots (**A** and **B**), whereas π-π interactions are displayed in cyan (**A**). Only polar hydrogens are shown for clarity. (For interpretation of the references to colour in this figure legend, the reader is referred to the Web version of this article.)

3.3. *In vivo evaluation of N-arachidonoyl conjugate production in the brain and assessment of the antinociceptive action of selected primary amines*

The primary amines (Fig. 1) were administered intraperitoneally (100 mg kg^{-1} or 300 mg kg^{-1}) to mice to examine their capacity to reach the brain and undergo FAAH-dependent fatty acid conjugation *in vivo* (Fig. 5A). The conjugations of **2**, **3**, 4-AP and HMBA, but not **1** and **4**, were FAAH-dependent, and the content of each *N*-arachidonoyl conjugate was different from that of AM404 in $FAAH^{+/+}$ mice (Fig. 5A, Table 3). The biotransformation of HMBA and **4** into their corresponding *N*-arachidonoyl conjugates was near the detection limit, as also previously reported for HMBA [18]. Therefore, compounds **2** and **3**, displaying compatible interactions with both FAAH and TRPV1 *in vitro*/*in vivo*, were evaluated for their antinociceptive properties. Compounds **2** (Fig. 5B and C) and **3** (Fig. 5D and E) displayed dose-dependent antinociceptive properties in the formalin test, and at doses that were without effect on locomotor activity (Fig. 5F). Furthermore, the blood-brain-barrier impermeable FAAH inhibitor, URB937, and the TRPV1 antagonist capsazepine were injected intracerebroventricularly to investigate if the antinociceptive effect of compounds **2** and **3** was dependent on brain FAAH and TRPV1 (Fig. 6). This restrictive pharmacologic intervention inhibited the antinociceptive effects of **2** and **3** during the second (Fig. 6B,D and F,H), but not the first (Fig. 6A,C and E,G), phase of the formalin test.

3.4. *Antipyretic effects of paracetamol and its FAAH substrate analogues*

To reveal any antipyretic effect of the antinociceptive FAAH substrate analogues of paracetamol, we compared the ability of 4-AP and the most efficient antinociceptive analogue **3** with that of paracetamol to reduce fever. Mice were pretreated with either lipopolysaccharide (LPS; 100 μg kg^{-1} i.p.) to induce fever or injected with saline (controls) and then exposed to drugs or vehicle in an *in vivo* model for telemetric temperature recordings to monitor the body temperature (Fig. 7). While paracetamol suppressed the fever at a dose of 100 mg kg^{-1} (Fig. 7A,A1), which is not antinociceptive in the mouse formalin test [17], the antinociceptive dose of 4-AP (30 mg kg^{-1}) was unable to attenuate the LPS-induced fever (Fig. 7B,B1). Febrile animals exposed to **3** at an antinociceptive dose (25 mg kg^{-1}) displayed a rapid decrease in core body temperature (Fig. 7C,C1).

The ability of the FAAH substrates 4-AP and **3** to reduce prostanoid synthesis in the diencephalon was investigated in mice rendered febrile with lipopolysaccharide (LPS; 100 μg kg^{-1} i.p.). Animals were sacrificed at a time-point (40 min) corresponding to the second nociceptive phase of the formalin test, which is also when paracetamol is most effective as antipyretic [37], and the diencephalic content of prostaglandin E2 (PGE_2), prostaglandin F2α ($PGF_{2\alpha}$), 6-keto-prostaglandin F1α (6-keto-$PGF_{1\alpha}$), and thromboxane B2 (TXB_2) was analyzed by LC-MS/MS (Table 4). 4-AP (30 mg kg^{-1}) partially inhibited the prostanoid elevations, although it was not antipyretic (Fig. 7), whereas immune-challenged mice treated with a non-antinociceptive dose of paracetamol (100 mg kg^{-1}), which caused complete extinction of the fever response (Fig. 7), showed substantially reduced levels of prostanoids (Table 4). To further study if the paracetamol/4-AP/FAAH metabolite AM404 mediates the antipyretic effect of paracetamol via COX inhibition, we investigated whether a previously established antipyretic dose of paracetamol [37] was able to inhibit the prostanoid synthesis in the diencephalon of immune challenged wild-type and FAAH-deficient mice. Measurements of the diencephalic prostanoid content indicated that paracetamol at 150 mg kg^{-1} equally inhibited prostanoid synthesis in both wild-type and FAAH-deficient mice (Table 4). Finally, the FAAH substrate compound **3** did not suppress the LPS-induced elevation of prostanoid levels in the diencephalon of febrile mice (Table 4), although it quickly reversed the febrile response (Fig. 7), indicating a COX-independent temperature reducing action.

3.5. *Evaluation of liver-toxic effects*

High paracetamol doses deplete the hepatic stores of protective glutathione which allows NAPQI to bind liver proteins and ultimately cause liver necrosis. We therefore tested 4-AP, HMBA, **2** and **3** in a mouse model for paracetamol-induced liver injury to evaluate the potential liver toxicity of these primary amines. Paracetamol (300 mg kg^{-1}, i.p.) created prominent centrilobular necrosis (Fig. 8A). These histological characteristics were not observed in livers from animals treated with an intraperitoneal injection of either 4-AP, HMBA, **2** or **3** at 300 mg kg^{-1} (Fig. 8B–E). The levels of hepatic alanine aminotransferase (ALT) and aspartate aminotransferase (AST), as well as the ratio between these aminotransferases, were also evaluated in the same animals to disclose potential

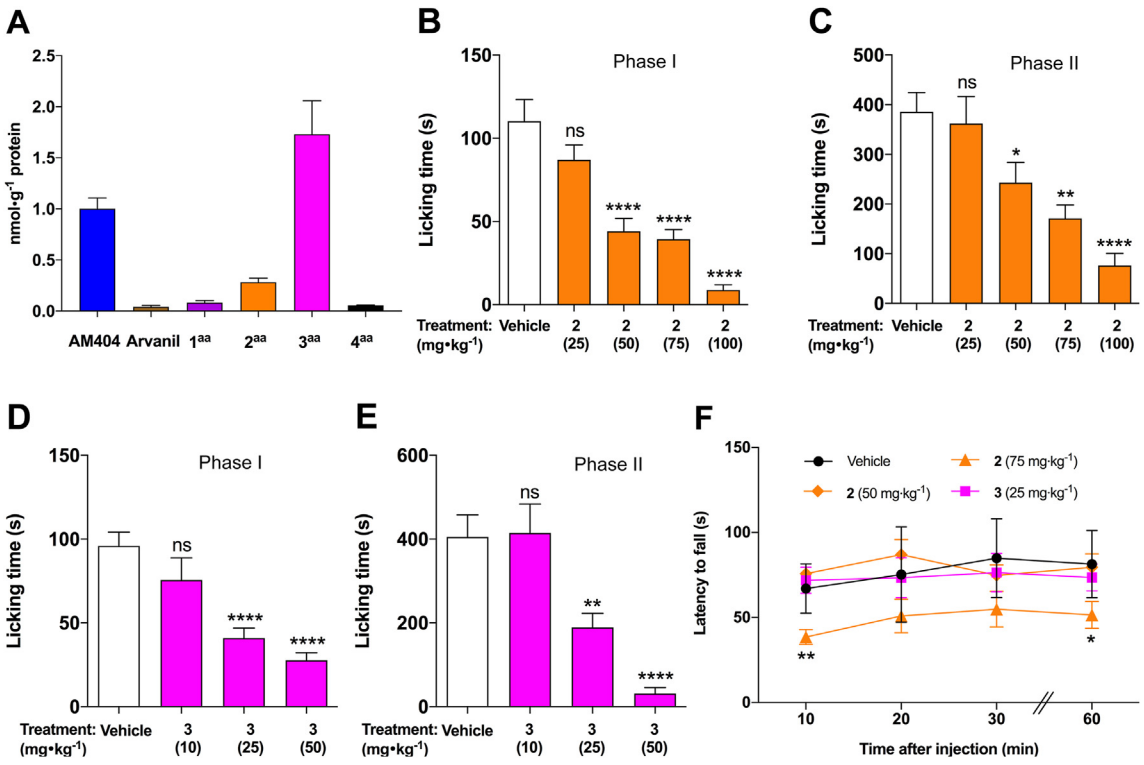

Fig. 5. *In vivo* brain production of TRPV1 active *N*-arachidonoyl conjugates from primary amines and their antinociceptive effects. (**A**) The brain content of AM404, arvanil and the *N*-arachidonoyl conjugates of compounds **1**–**4** (denoted with ^{aa}) were determined in brain from wild-type mice 20 min after intraperitoneal administration of the corresponding primary amine. The production of $\mathbf{2}^{aa}$ and $\mathbf{3}^{aa}$, but not $\mathbf{1}^{aa}$ and $\mathbf{4}^{aa}$, were FAAH-dependent (Table 3). Compared to AM404 ($n = 9$), the content of each other *N*-arachidonoyl conjugate was different in FAAH$^{+/+}$ mice [$P < 0.01$ for arvanil ($n = 3$), $P < 0.001$ for $\mathbf{1}^{aa}$ ($n = 7$), $P < 0.01$ for $\mathbf{2}^{aa}$ ($n = 6$), $\mathbf{3}^{aa}$ ($n = 8$) and $\mathbf{4}^{aa}$ ($n = 4$) as determined by 1-way ANOVA followed by Sidak's multiple comparisons test]. Except for HMBA, of which the corresponding *N*-arachidonoyl conjugate arvanil only was detected at 300 mg kg^{-1}, the other primary amines were administered at a dose of 100 mg kg^{-1}. (**B**–**E**) The primary amines **2** and **3** were further assessed for antinociceptive properties in the formalin test. Both **2** and **3** displayed antinociceptive properties during the first (**B** and **D**) and second phase (**C** and **E**), respectively, of the formalin test (*$P < 0.05$, **$P < 0.01$, ****$P < 0.0001$ determined by 1-way ANOVA followed by Dunnett's multiple comparisons test; $n = 5$–6). Vehicle, **2** or **3** were injected intraperitoneally 10 min before the formalin test. (**F**) Effect of **2**, **3** and vehicle on locomotor ability measured continuously in the rotarod test at different time points after intraperitoneal administration. A rotating drum was accelerated from 4 to 40 revolutions per minute over the course of 5 min and the time point at which the mouse fell off the rod was recorded (Latency to fall). *$P < 0.05$ and **$P < 0.01$ for vehicle vs **2** (75 mg kg^{-1}) [Repeated measures two-way ANOVA followed by Dunnett's multiple comparisons test, $n = 8$]. Data are presented as mean ± SEM.

Table 3
In vivo fatty acid conjugation of primary amines by FAAH into *N*-arachidonoyl conjugates.

Compound	*N*-arachidonoyl conjugates (pmol g^{-1} protein)			
	FAAH$^{+/+}$	*n*	FAAH$^{-/-}$	*n*
4-AP	1002 ± 106	9	24 ± 12	3
HMBA	40 ± 13	3	n.d.	3
1	82 ± 22	7	190 ± 90	4
2	283 ± 39	6	42 ± 5	3
3	1731 ± 328	8	161 ± 50	4
4	58 ± 0.3	4	58 ± 0.5	3

The fatty acid amide hydrolase (FAAH) *in vivo* activity was determined in brains obtained from FAAH$^{+/+}$ or FAAH$^{-/-}$ mice 20 min after intraperitoneal injection (i.p.) of the primary amine (Compound). Except for HMBA, of which the corresponding *N*-arachidonoyl conjugate arvanil was only detected at a higher dose of HMBA (300 mg kg^{-1}), each other primary amine was administered at a dose of 100 mg kg^{-1}. The content of *N*-arachidonoyl conjugates in FAAH$^{+/+}$ vs FAAH$^{-/-}$ mice was compared with significant differences obtained for 4-AP ($P < 0.01$, 1-way ANOVA followed by Sidak's multiple comparisons test), **2** and **3** ($P < 0.01$) but not **1** and **4** using the Student's unpaired *t*-test. Compared to AM404, the content of each other *N*-arachidonoyl conjugate was different in FAAH$^{+/+}$ mice (see also Fig. 5A). Data are presented as mean ± SEM, and *n* denotes the number of animals. n.d. = not detected.

hepatoxicity of the primary amines (Fig. 8F and G). Statistical analysis revealed significant differences in ALT levels between paracetamol and either of 4-AP, HMBA, **2** or **3** (Fig. 8F). Although no histological changes were noted for 4-AP (Fig. 8B), it increased the ALT/AST ratio close to 1 (Fig. 8G).

4. Discussion

The objective of this study was to explore the structure-activity relationship of paracetamol and primary amine analogues with regard to their ability to undergo a FAAH-dependent biotransformation into *N*-arachidonoyl conjugates mediating TRPV1-induced antinociception. To exploit differences in the FAAH-mediated conjugation of primary amines and the TRPV1 efficacy of their corresponding *N*-arachidonoyl conjugates, a computational analysis guided by the outcome from our initial *in vitro* functional studies of FAAH and TRPV1 activity was undertaken. Thus, we first performed a computational study of the interaction between FAAH and the *N*-arachidonoyl conjugates of compounds **2** and **3** compared with the paracetamol metabolite AM404. The covalently linked tetrahedral FAAH-intermediate of the corresponding *N*-arachidonoyl conjugate of **3** had a low-energy conformation with a planar sp2-hybridised amide nitrogen in FAAH, while the corresponding covalently linked FAAH-intermediate of AM404 and **2** had pyramidal amide nitrogens in the energy-minimized complexes. These observations, together with the *in vitro* findings of FAAH-mediated conjugation of compounds **2**, **3** and 4-AP, suggest that the amount of *N*-arachidonoyl conjugate produced may be related to the geometry of its amide nitrogen in the covalently linked

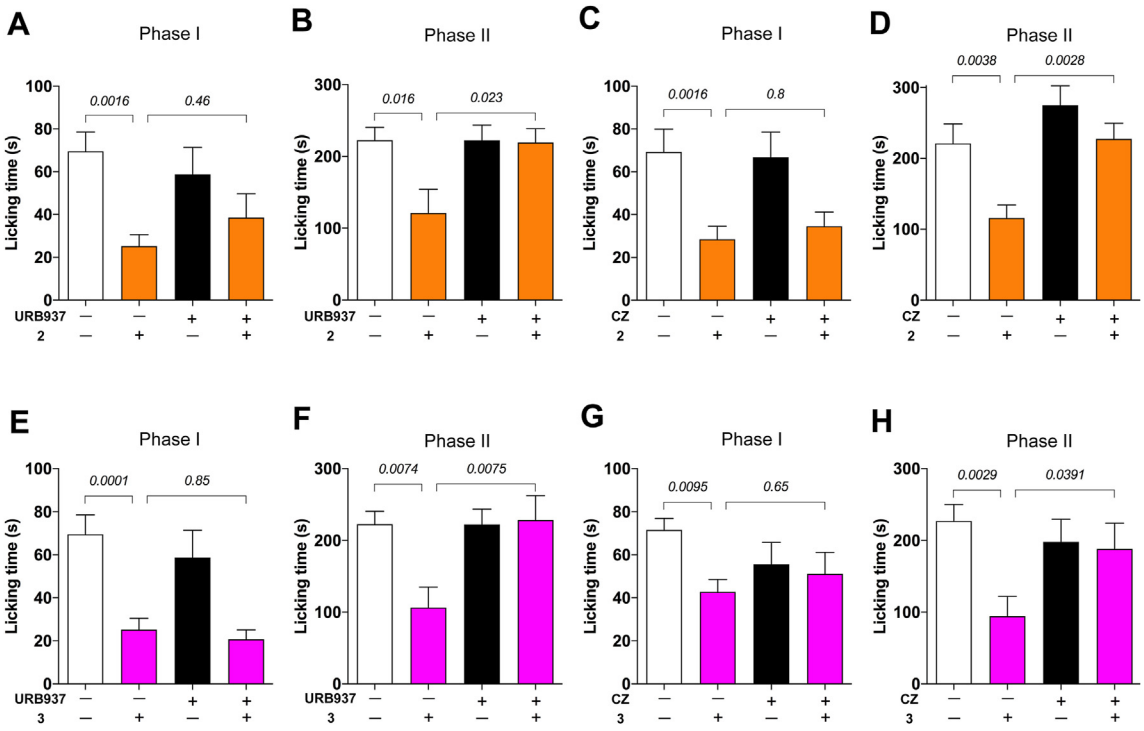

Fig. 6. The role of brain FAAH and TRPV1 in the antinociceptive effect of compounds **2** and **3**. Whereas pre-treatment with the FAAH inhibitor URB937 (5 μg in 5 μl, i.c.v.) had no effect on the antinociception of **2** (50 mg kg^{-1}, i.p) and **3** (25 mg kg^{-1}, i.p.) during the first phase of the formalin test (**A** and **E**) it attenuated the antinociception during the second phase (**B** and **F**). In a similar manner, the TRPV1 antagonist capsazepine (CZ) (10 μg in 5 μl, i.c.v.) attenuated the antinociception of **2** and **3** during the second phase (**D** and **H**) but had no effect during the first phase (**C** and **G**). The statistical comparisons in the graph were performed between mice treated with a compound (−/+) and non-treated mice (−/−) as well as between mice treated with a compound (−/+) and mice treated with both compound and antagonist (+/+) using 1-way ANOVA followed by Dunnett's multiple comparisons test (*P* values in italics). All i.c.v. injections were performed 5 min before i.p. administration of **2** or **3**. Data are presented as mean ± SEM (n = 8–14). ns = not significant.

FAAH-intermediate. However, further experiments are needed to consolidate a causal relationship for this observation. The computational studies of AM404 and TRPV1 disclosed that the hydroxyl group enables key interactions with Arg557 and Glu570, which is in line with recent findings [44] and points to a putative link towards the TRP-domain (represented by Gln700), a structure important for the potency and specificity of vanilloid ligands [42,45–47]. Interestingly, when the distance between the hydrogen donating and accepting atom of this hydroxyl group was increased/separated by the presence of an extra heteroatom in **2** and **3**, *i.e.* the hydroxy and methoxy groups in **2** and the two nitrogens of the indazole moiety in **3**, the TRPV1 potency of the corresponding *N*-arachidonoyl analogues was increased. Hypothetically, these moieties better resemble the vanilloid head group of the potent TRPV1 activators capsaicin and resiniferatoxin and possess more optimized interactions towards Arg557 and Glu570. Our findings indicate that aliphatic amines form *N*-arachidonoyl conjugates with higher TRPV1 potency than aromatic amines, but are poorly biotransformed by FAAH yielding low amounts of their corresponding *N*-arachidonoyl conjugates. However, the low yield of such *N*-arachidonoyl conjugates are not necessarily caused by steric hindrance, since FAAH is able to accommodate larger and more complex structures. Thus, additional computational studies are needed in order to develop new analogues with better FAAH interface. In this context, structural variations of compounds **2** and **3** that do not lead to major steric or geometric alteration may be interesting further developments of these two compounds.

Even though the *N*-arachidonoyl conjugates of **1** and **4** were full agonists and more potent than AM404 as activators of TRPV1, their *in vivo* transformation into corresponding *N*-arachidonoyl conjugates was independent of FAAH, and we therefore chose to investigate the antinociceptive properties of **2** and **3** with regard to supraspinal FAAH and TRPV1 dependence. Compounds **2** and **3** demonstrated dose-dependent antinociceptive properties in the two phases of the formalin test, suggesting that their antinociceptive profile resembles that of paracetamol and is different from that of commonly used NSAIDs [17,48]. Interestingly, compound **3** showed an antinociceptive efficacy at least twice as high as compound **2,** most likely because **3** is a better substrate for FAAH. Furthermore, compounds **2** and **3** showed an antinociceptive profile that was associated with functional FAAH- and TRPV1-mediated actions in the brain. These effects were, however, restricted to the second phase of the formalin test as FAAH and TRPV1 inhibition by the i.c.v. administration of URB937 and capsazepine, respectively, did not prevent the inhibition of the nociceptive response during first phase of the formalin test in contrast to what has been reported when animals are given paracetamol, 4-AP or HMBA [17,18]. Since URB937 and capsazepine were administered at well-established doses these differences may be best explained by additional FAAH and TRPV1-independent antinociceptive mechanisms of compounds **2** and **3**.

The antipyretic action of paracetamol has been attributed to inhibition of central COX [36,49], and the *N*-arachidonoyl conjugate AM404, which is produced by FAAH from paracetamol-derived 4-AP, has been shown to inhibit COX-mediated production of the pyrogenic mediator PGE_2 *in vitro* [16,27]. We therefore compared the antipyretic effects of compound **3**, which was the most efficient FAAH-dependent antinociceptive paracetamol analogue, and 4-AP with the antipyretic effect of paracetamol. Interestingly, when given at doses that produced antinociception, compound **3** reversed the febrile response in mice, whereas 4-AP had no effect. To better understand the temperature regulating effects of **3** with

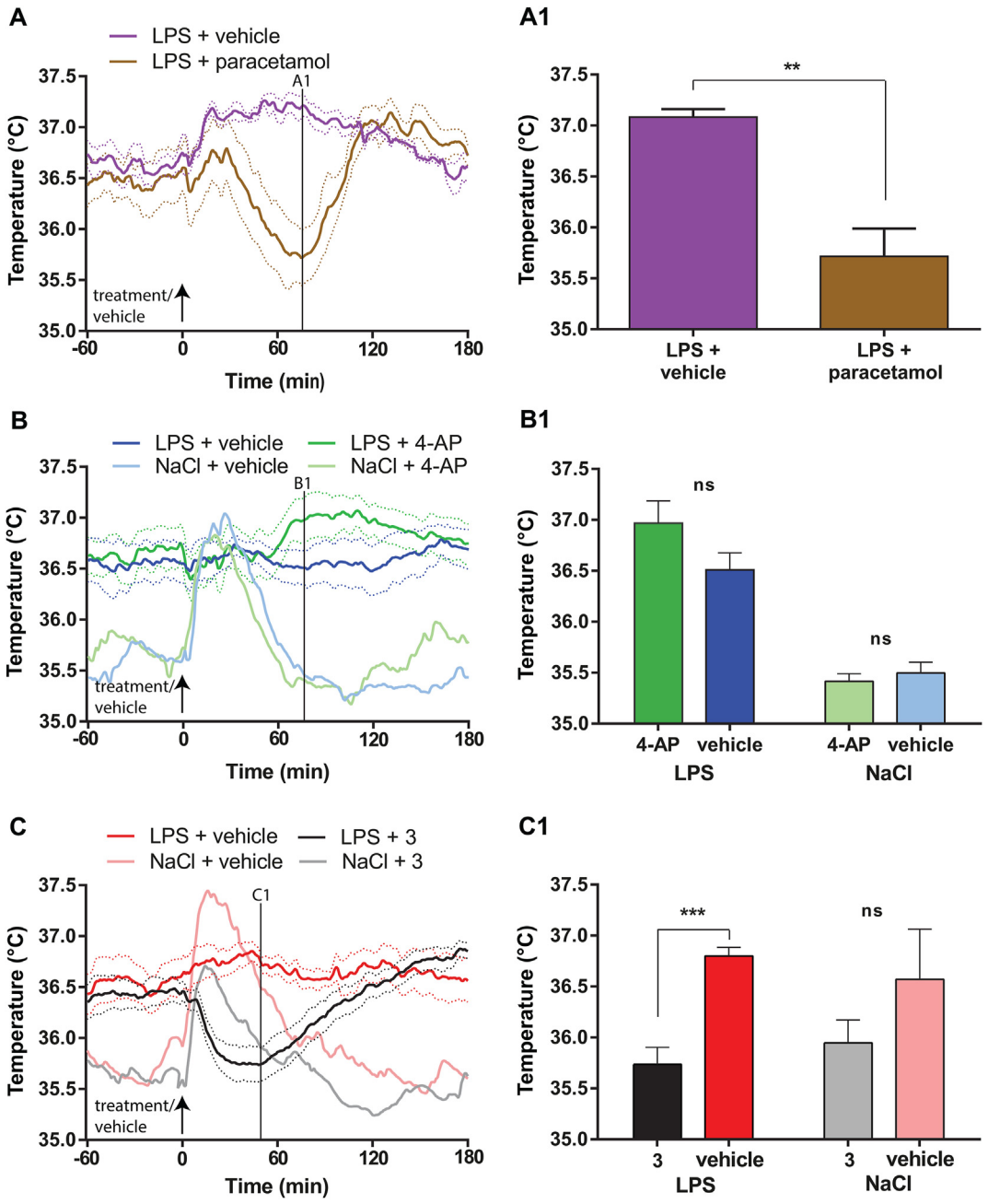

Fig. 7. Antipyretic effects of paracetamol and analogues. (**A**) Mice were rendered febrile by immune challenge with LPS (100 μg kg^{-1} i.p.) and treated with a sub-antinociceptive dose of paracetamol (100 mg kg^{-1} i.p.) or injected with vehicle. The solid temperature traces represent the mean, and dotted lines SEM ($n = 6$ for LPS + paracetamol injected mice and $n = 4$ for LPS + vehicle injected mice). (**A1**) Statistical analysis of values at the nadir of the antipyretic effect of paracetamol (**A1**, $T_{nadir} = 75$ min after treatment with paracetamol; *t*-test: $P = 0.0043$ for LPS + vehicle vs LPS + paracetamol). (**B**) Mice were rendered febrile by immune challenge with LPS (100 μg kg^{-1} i.p.; upper two traces) or given saline (lower two traces) and treated with an anti-nociceptive dose of 4-AP (30 mg kg^{-1} i.p.) or vehicle. Injecting non-febrile mice resulted in a transient handling stress-induced hyperthermia, irrespective of whether 4-AP or vehicle was given. As seen 4-AP had no temperature lowering effect on febrile mice. The solid temperature traces represent the mean, and dotted lines SEM ($n = 8$ for LPS treated animals, and $n = 4$ for saline treated animals). (**B1**) Statistical analysis of values at the time point corresponding to nadir for the antipyretic effect of paracetamol (see **A**; 2-way ANOVA followed by Sidak's multiple comparisons test) ns = not significant. (**C**) Mice were rendered febrile by immune challenge with LPS (100 μg kg^{-1} i.p.; upper two traces) or given saline (lower two traces) and treated with an anti-nociceptive dose of **3** (25 mg kg^{-1} i.p.) or vehicle. Except for the handling-stress induced hyperthermia, the administration of **3** to non-febrile animals had no intrinsic effects on body temperature, whereas **3** given to febrile mice resulted in a rapid temperature fall. The solid temperature traces represent the mean, and dotted lines SEM ($n = 9$ for LPS injected animals, and $n = 4$ for saline injected animals). (**C1**) Statistical analysis of values at the nadir of the antipyretic effect of **3** (**C1**, $T_{nadir} = 48$ min after administration of **3**; 2-way ANOVA followed by Sidak's multiple comparisons test: $F_{1,22} = 14.31$, $P = 0.0010$; $P = 0.0006$ for LPS + vehicle vs LPS + **3**). ns = not significant.

regard to pyrexia, we performed additional experiments determining brain prostanoid levels in febrile mice. The effects of the antipyretic paracetamol and the non-antipyretic 4-AP were also studied. In line with our recent findings [37], paracetamol decreased the prostanoid levels in the diencephalon and attenuated the pyrexia in immune challenged mice at a dose that is not antinociceptive (100 mg kg^{-1}). Interestingly, an antinociceptive dose of 4-AP (30 mg kg^{-1}) partially reduced the LPS-induced elevation of prostanoids in the diencephalon, but, as reported above, it did not affect the febrile response. Furthermore,

Table 4
Effect of paracetamol, 4-AP and 3 on LPS-induced prostanoid levels in mouse diencephalon.

Treatment	PGE_2	$PGF_{2\alpha}$	6-keto-$PGF_{1\alpha}$	TXB_2
Paracetamol (100 mg kg^{-1})	13 ± 5	18 ± 1	17 ± 5	36 ± 5
4-AP (30 mg kg^{-1})	44 ± 9	81 ± 8	60 ± 10	60 ± 23
3 (25 mg kg^{-1})	96 ± 7	100 ± 6	99 ± 4	91 ± 5
Paracetamol (150 mg kg^{-1}) $FAAH^{+/+}$	8 ± 2	19 ± 4	15 ± 3	25 ± 3
Paracetamol (150 mg kg^{-1}) $FAAH^{-/-}$	9 ± 3	10 ± 3	12 ± 2	18 ± 6

The inhibition of COX was evaluated by analysing the content of prostanoids in diencephalon from mice immune challenged with LPS (100 μg kg^{-1}) or saline, administered intraperitoneally (i.p.) 3 h prior to treatment for 40 min with paracetamol, 4-AP, **3** or their vehicle ($n = 6$). $P < 0.0001$ (PGE_2, $PGF_{2\alpha}$ and 6-keto-$PGF_{1\alpha}$), $P < 0.01$ (TXB_2) for paracetamol vs vehicle (control). $P < 0.0001$ (PGE_2), $P < 0.05$ ($PGF_{2\alpha}$), $P < 0.001$ (6-keto-$PGF_{1\alpha}$) for 4-AP vs vehicle (control). No difference in prostanoid contents was observed after treatment with **3**. Statistical significance was accepted when $P < 0.05$ (1-way ANOVA followed by Dunnett's multiple comparisons test). The prostanoid assay was also used in a separate set of experiments to evaluate the ability of paracetamol (150 mg kg^{-1} i.p.) to inhibit COX in $FAAH^{+/+}$ ($n = 10–11$) and $FAAH^{-/-}$ ($n = 5$) mice. No difference was observed in the prostanoid content between FAAH genotypes ($P > 0.1$, Student's unpaired t-test). Values are calculated as a percentage of those obtained in febrile animals treated with compound vehicle. Data are presented as mean ± SEM.

compound **3** did not suppress the LPS-induced elevation of prostanoid levels in the diencephalon of febrile mice, and thus the rapid decrease in core body temperature mediated by **3** is unrelated to inhibition of supraspinal COX synthesis of prostanoids. An acetylated analogue of **3** has been shown to selectively inhibit COX-2 in certain experiments indicating that minor modifications of aminoindazole compounds may counteract febrile responses by multiple mechanisms [50]. The findings that compound **3** in the present study and 4-AP [18] at antinociceptive doses did not cause hypothermia in non-febrile animals and that they did not affect locomotor activity in mice are also important observations as hypothermia is known to affect the antinociceptive readout in animal behavioral studies. Finally, paracetamol was able to equally prevent LPS-induced prostanoid synthesis in the diencephalon of wild-type and FAAH deficient mice, demonstrating that the supraspinal COX inhibition mediated by paracetamol occurs independent of FAAH. Thus, the antipyretic effect of paracetamol, in contrast to its antinociceptive effect [17,25], is not mediated by AM404. Consequently, future therapies that utilize the potential dichotomy between the antipyretic and antinociceptive effects of paracetamol may be of value as fever is presumably beneficial by enhancing the capacity of the immune system while impairing pathogens [51].

One of the major drawbacks with paracetamol is its degradation into the liver-toxic metabolite NAPQI. Although our analogues **2** and **3** may be less prone to form such electrophilic species, the full molecular mechanism of acetaminophen-induced hepatotoxicity is still unclear. While pharmacological inhibition of TRPV1 did not alleviate acetaminophen-induced hepatotoxicity [52], a recent publication showed that TRPV4 inhibitors are able to reduce paracetamol-induced necrosis in primary human hepatocytes [53]. To evaluate liver toxicity, we performed biochemical and histological liver examinations of animals exposed to paracetamol, 4-AP, HMBA, **2** or **3**. We found that 4-AP, HMBA, **2** and **3** did not induce a paracetamol-like hepatotoxicity at a dose at which paracetamol produces a robust injury. 4-AP caused a borderline risk ALT/AST ratio >1, perhaps by conversion into its *p*-benzoquinone metabolite or by acetylation into paracetamol [54,55].

5. Conclusions

In this study, we have combined *in vitro*/*in vivo* studies of FAAH and TRPV1 activity with computational studies to understand the

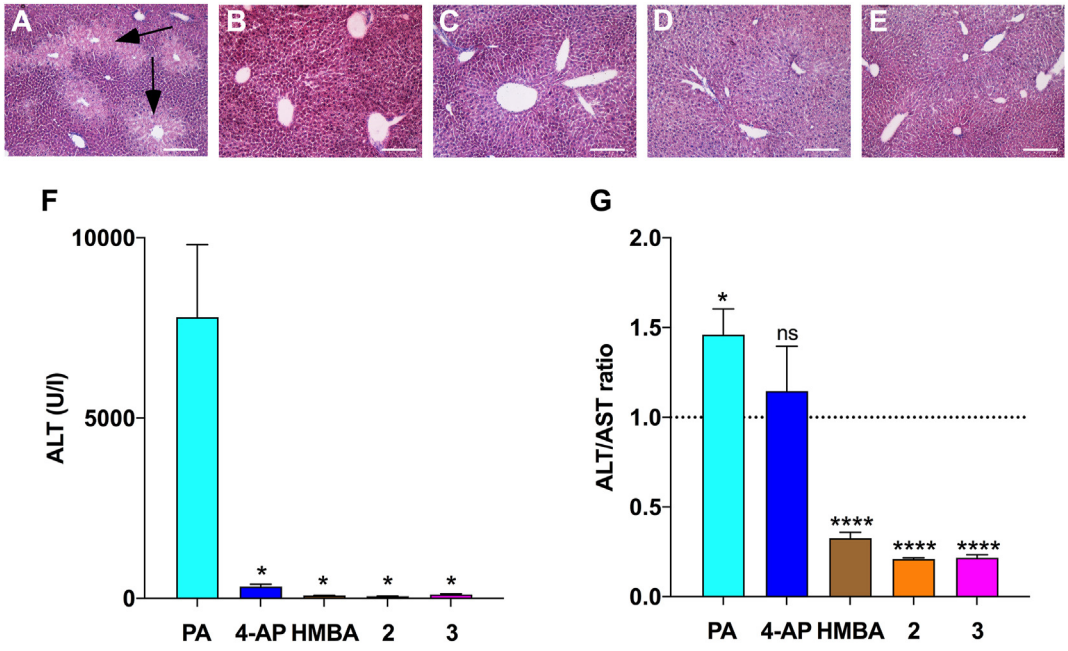

Fig. 8. Evaluation of liver injury. Male C57/BL6 mice were fasted for 12–16 h before receiving an intraperitoneal injection of 300 mg kg^{-1} paracetamol, 4-AP, HMBA, **2** or **3**. Serum samples and liver tissues were collected 12 h after administration. (**A**–**E**) Micrographs of liver samples from paracetamol (**A**), 4-AP (**B**), HMBA (**C**), **2** (**D**) and **3** (**E**) treated animals, stained with haematoxylin and eosin. Necrotic areas are visualized as lighter zones surrounding hepatic vessels (arrows). Scale bar = 200 μm. (**F**) The liver damage created by paracetamol is associated with increased hepatic alanine aminotransferase (ALT) levels. The ALT levels were significantly higher after exposure to paracetamol compared to those seen after exposure to 4-AP (*$P = 0.0139$), HMBA (*$P = 0.0122$), **2** (*$P = 0.0121$) and **3** (*$P = 0.0124$) as determined by the Welch's ANOVA test. (**G**) A ratio between ALT and aspartate aminotransferase (AST) > 1 is a clinical marker for hepatic injury. Paracetamol and 4-AP increased this ratio close to 1 (4-AP) and above (paracetamol, *$P = 0.0191$), whereas the ratios for HMBA, **2** and **3** were far below 1 (****$P < 0.0001$); One sample t-test compared to the ratio of 1 (ns = not significant). Data are presented as mean ± SEM ($n = 6–7$).

structure-activity relationship of paracetamol and primary amine analogues thereof at FAAH and TRPV1, with the aim to find paracetamol analogues that are antinociceptive at lower doses and without acute liver toxicity. We found that the *N*-arachidonoyl conjugates of 5-amino-2-methoxyphenol (**2**) and 5-aminoindazole (**3**) displayed efficient target protein interactions with FAAH and TRPV1, and possessed a dose-dependent antinociception in both phases of the formalin test that during the second phase was mediated by FAAH and TRPV1 in the brain of mice. Importantly, none of the compounds demonstrated hepatotoxicity. We also demonstrate that the antipyretic COX inhibitory action of paracetamol, in contrast to its antinociceptive mechanism, does not involve FAAH-dependent biotransformation of paracetamol into its *N*-arachidonoyl conjugate AM404. Furthermore, compound **3** reduced fever without inhibiting prostanoid formation in the brain, suggesting a COX-independent mechanism. Our study shows that analgesics and antipyretics without liver toxicity can be derived from paracetamol. Thus, further research into the molecular actions of paracetamol could pave the way for the discovery of analgesics and antipyretics with a better benefit-to-risk ratio.

Author contributions

J.L.Å.N, E.D.H[†]. and P.M.Z. conceived, designed and directed the study; C.M. and L.B. conducted nociceptive tests; J.L.Å.N. conducted the biochemical *in vitro* and *in vivo* experiments; A.B-n. performed the mass spectrometry analyses; J.L.Å.N., A.P.S. and U.J.N. performed and interpreted computational studies; K.S. and A.B-t performed the telemetric recordings of body temperature; J.L.Å.N, A.B-t, C.M., A.E and P.M.Z. analyzed data; J.L.Å.N, A.B-t, C.M., A.E., U.J.N and P.M.Z wrote the manuscript. All authors discussed the results and revised or commented on the manuscript. [†]Edward Dag Högestätt (E.D.H.) deceased.

Declaration of competing interest

The authors declare that they have no known competing financial interests or personal relationships that could have appeared to influence the work reported in this paper.

Acknowledgements

This study was supported by Medical Faculty of Lund University (Dnr. ALFSKANE-450751), AFA Försäkring (Dnr. 140376), Hjärnfonden (FO2019-0316), Stiftelsen Olle Engkvist Byggmästare (189–290), The Swedish Research Council (#07879) and The Royal Physiographic Society, Lund Sweden, Clermont Auvergne University, INSERM and the Agence Nationale de la Recherche of the French government through the program "Investissements d'Avenir" (I-Site CAP 20–25).

References

[1] M. Blieden, L.C. Paramore, D. Shah, R. Ben-Joseph, A perspective on the epidemiology of acetaminophen exposure and toxicity in the United States, Expet Rev. Clin. Pharmacol. 7 (2014) 341–348, https://doi.org/10.1586/17512433.2014.904744.

[2] J.W. Wastesson, J.E. Martikainen, H. Zoëga, M. Schmidt, Ø. Karlstad, A. Pottegård, Trends in use of paracetamol in the nordic countries, Basic Clin. Pharmacol. Toxicol. 123 (2018) 301–307, https://doi.org/10.1111/bcpt.13003.

[3] G.C. Machado, C.G. Maher, P.H. Ferreira, M.B. Pinheiro, C.W. Lin, R.O. Day, A.J. McLachlan, M.L. Ferreira, Efficacy and safety of paracetamol for spinal pain and osteoarthritis: systematic review and meta-analysis of randomised placebo controlled trials, BMJ 350 (2015) h1225.

[4] Z.N. Ennis, D. Dideriksen, H.B. Vaegter, G. Handberg, A. Pottegård, Acetaminophen for chronic pain: a systematic review on efficacy, Basic Clin. Pharmacol. Toxicol. 118 (2016) 184–189, https://doi.org/10.1111/bcpt.12527.

[5] R.R. Bannuru, M.C. Osani, E.E. Vaysbrot, N.K. Arden, K. Bennell, S.M.A. Bierma-Zeinstra, V.B. Kraus, L.S. Lohmander, J.H. Abbott, M. Bhandari, F.J. Blanco, R. Espinosa, I.K. Haugen, J. Lin, L.A. Mandl, E. Moilanen, N. Nakamura, L. Snyder-Mackler, T. Trojian, M. Underwood, T.E. McAlindon, OARSI guidelines for the non-surgical management of knee, hip, and polyarticular osteoarthritis, Osteoarthritis Cartilage 27 (2019) 1578–1589, https://doi.org/10.1016/j.joca.2019.06.011.

[6] S.L. Kolasinski, T. Neogi, M.C. Hochberg, C. Oatis, G. Guyatt, J. Block, L. Callahan, C. Copenhaver, C. Dodge, D. Felson, K. Gellar, W.F. Harvey, G. Hawker, E. Herzig, C.K. Kwoh, A.E. Nelson, J. Samuels, C. Scanzello, D. White, B. Wise, R.D. Altman, D. DiRenzo, J. Fontanarosa, G. Giradi, M. Ishimori, D. Misra, A.A. Shah, A.K. Shmagel, L.M. Thoma, M. Turgunbaev, A.S. Turner, J. Reston, American college of rheumatology/arthritis foundation guideline for the management of osteoarthritis of the hand, hip, and knee, Arthritis Rheum. 72 (2020) (2019) 220–233, https://doi.org/10.1002/art.41142.

[7] C.M. Williams, C.G. Maher, J. Latimer, A.J. McLachlan, M.J. Hancock, R.O. Day, C.W. Lin, Efficacy of paracetamol for acute low-back pain: a double-blind, randomised controlled trial, Lancet 384 (2014) 1586–1596, https://doi.org/10.1016/S0140-6736(14)60805-9.

[8] G. Pickering, I. Creveaux, N. Macian, B. Pereira, Paracetamol and pain modulation by TRPV1, UGT2B15, SULT1A1 genotypes: a randomized clinical trial in healthy volunteers, Pain Med. 21 (2020) 661–669, https://doi.org/10.1093/pm/pnz037.

[9] K. Heard, J.L. Green, V. Anderson, B. Bucher-Bartelson, R.C. Dart, Paracetamol (acetaminophen) protein adduct concentrations during therapeutic dosing, Br. J. Clin. Pharmacol. 81 (2016) 562–568, https://doi.org/10.1111/bcp.12831.

[10] P.B. Watkins, N. Kaplowitz, J.T. Slattery, C.R. Colonese, S.V. Colucci, P.W. Stewart, S.C. Harris, Aminotransferase elevations in healthy adults receiving 4 grams of acetaminophen daily: a randomized controlled trial, J. Am. Med. Assoc. 296 (2006) 87–93, https://doi.org/10.1001/jama.296.1.87.

[11] S. Shinoda, T. Aoyama, Y. Aoyama, S. Tomioka, Y. Matsumoto, Y. Ohe, Pharmacokinetics/pharmacodynamics of acetaminophen analgesia in Japanese patients with chronic pain, Biol. Pharm. Bull. 30 (2007) 157–161.

[12] A.M. Larson, J. Polson, R.J. Fontana, T.J. Davern, E. Lalani, L.S. Hynan, J.S. Reisch, F.V. Schiødt, G. Ostapowicz, A.O. Shakil, W.M. Lee, A.L.F.S. Group, Acetaminophen-induced acute liver failure: results of a United States multicenter, prospective study, Hepatology 42 (2005) 1364–1372, https://doi.org/10.1002/hep.20948.

[13] G. Wei, A. Bergquist, U. Broomé, S. Lindgren, S. Wallerstedt, S. Almer, P. Sangfelt, A. Danielsson, H. Sandberg-Gertzén, L. Lööf, H. Prytz, E. Björnsson, Acute liver failure in Sweden: etiology and outcome, J. Intern. Med. 262 (2007) 393–401, https://doi.org/10.1111/j.1365-2796.2007.01818.x.

[14] W. Bernal, J. Wendon, Acute liver failure, N. Engl. J. Med. 369 (2013) 2525–2534, https://doi.org/10.1056/NEJMra1208937.

[15] W.A. Bower, M. Johns, H.S. Margolis, I.T. Williams, B.P. Bell, Population-based surveillance for acute liver failure, Am. J. Gastroenterol. 102 (2007) 2459–2463, https://doi.org/10.1111/j.1572-0241.2007.01388.x.

[16] E.D. Hogestatt, B.A. Jonsson, A. Ermund, D.A. Andersson, H. Bjork, J.P. Alexander, B.F. Cravatt, A.I. Basbaum, P.M. Zygmunt, Conversion of acetaminophen to the bioactive N-acylphenolamine AM404 via fatty acid amide hydrolase-dependent arachidonic acid conjugation in the nervous system, J. Biol. Chem. 280 (2005) 31405–31412, https://doi.org/10.1074/jbc.M501489200.

[17] C. Mallet, D.A. Barrière, A. Ermund, B.A. Jönsson, A. Eschalier, P.M. Zygmunt, E.D. Högestätt, TRPV1 in brain is involved in acetaminophen-induced antinociception, PLoS One 5 (2010), https://doi.org/10.1371/journal.pone.0012748.

[18] D.A. Barrière, C. Mallet, A. Blomgren, C. Simonsen, L. Daulhac, F. Libert, E. Chapuy, M. Etienne, E.D. Högestätt, P.M. Zygmunt, A. Eschalier, Fatty acid amide hydrolase-dependent generation of antinociceptive drug metabolites acting on TRPV1 in the brain, PLoS One 8 (2013), e70690, https://doi.org/10.1371/journal.pone.0070690.

[19] D.A. Barriere, F. Boumezbeur, R. Dalmann, R. Cadeddu, D. Richard, J. Pinguet, L. Daulhac, P. Sarret, K. Whittingstall, M. Keller, S. Meriaux, A. Eschalier, C. Mallet, Paracetamol is a centrally acting analgesic using mechanisms located in the periaqueductal grey, Br. J. Pharmacol. (2019), https://doi.org/10.1111/bph.14934.

[20] C. Mallet, L. Daulhac, J. Bonnefont, C. Ledent, M. Etienne, E. Chapuy, F. Libert, A. Eschalier, Endocannabinoid and serotonergic systems are needed for acetaminophen-induced analgesia, Pain 139 (2008) 190–200, https://doi.org/10.1016/j.pain.2008.03.030.

[21] B.F. Cravatt, D.K. Giang, S.P. Mayfield, D.L. Boger, R.A. Lerner, N.B. Gilula, Molecular characterization of an enzyme that degrades neuromodulatory fatty-acid amides, Nature 384 (1996) 83–87, https://doi.org/10.1038/384083a0.

[22] P.M. Zygmunt, H. Chuang, P. Movahed, D. Julius, E.D. Högestätt, The anandamide transport inhibitor AM404 activates vanilloid receptors, Eur. J. Pharmacol. 396 (2000) 39–42.

[23] P.M. Zygmunt, A. Ermund, P. Movahed, D.A. Andersson, C. Simonsen, B.A. Jonsson, A. Blomgren, B. Birnir, S. Bevan, A. Eschalier, C. Mallet, A. Gomis, E.D. Hogestatt, Monoacylglycerols activate TRPV1–a link between phospholipase C and TRPV1, PLoS One 8 (2013), e81618, https://doi.org/10.1371/journal.pone.0081618.

[24] S. Maione, T. Bisogno, V. de Novellis, E. Palazzo, L. Cristino, M. Valenti, S. Petrosino, V. Guglielmotti, F. Rossi, V. Di Marzo, Elevation of endocannabinoid levels in the ventrolateral periaqueductal grey through inhibition of

fatty acid amide hydrolase affects descending nociceptive pathways via both cannabinoid receptor type 1 and transient receptor potential vanilloid type-1 receptors, J. Pharmacol. Exp. Therapeut. 316 (2006) 969–982, https://doi.org/10.1124/jpet.105.093286.
[25] R. Dalmann, L. Daulhac, M. Antri, A. Eschalier, C. Mallet, Supra-spinal FAAH is required for the analgesic action of paracetamol in an inflammatory context, Neuropharmacology 91 (2015) 63–70, https://doi.org/10.1016/j.neuropharm.2014.11.006.
[26] A. Fukushima, K. Mamada, A. Iimura, H. Ono, Supraspinal-selective TRPV1 desensitization induced by intracerebroventricular treatment with resiniferatoxin, Sci. Rep. 7 (2017) 12452, https://doi.org/10.1038/s41598-017-12717-5.
[27] S.W. Saliba, A.R. Marcotegui, E. Fortwängler, J. Ditrich, J.C. Perazzo, E. Muñoz, A.C.P. de Oliveira, B.L. Fiebich, AM404, paracetamol metabolite, prevents prostaglandin synthesis in activated microglia by inhibiting COX activity, J. Neuroinflammation 14 (2017) 246, https://doi.org/10.1186/s12974-017-1014-3.
[28] C.V. Sharma, J.H. Long, S. Shah, J. Rahman, D. Perrett, S.S. Ayoub, V. Mehta, First evidence of the conversion of paracetamol to AM404 in human cerebrospinal fluid, J. Pain Res. 10 (2017) 2703–2709, https://doi.org/10.2147/JPR.S143500.
[29] M. Mileni, J. Garfunkle, C. Ezzili, B.F. Cravatt, R.C. Stevens, D.L. Boger, Fluoride-mediated capture of a noncovalent bound state of a reversible covalent enzyme inhibitor: X-ray crystallographic analysis of an exceptionally potent α-ketoheterocycle inhibitor of fatty acid amide hydrolase, J. Am. Chem. Soc. 133 (2011) 4092–4100, https://doi.org/10.1021/ja110877y.
[30] Y. Gao, E. Cao, D. Julius, Y. Cheng, TRPV1 structures in nanodiscs reveal mechanisms of ligand and lipid action, Nature 534 (2016) 347–351, https://doi.org/10.1038/nature17964.
[31] M. Zimmermann, Ethical guidelines for investigations of experimental pain in conscious animals, Pain 16 (1983) 109–110.
[32] C. Kilkenny, W. Browne, I.C. Cuthill, M. Emerson, D.G. Altman, N.C.R.R.G.W. Group, Animal research: reporting in vivo experiments: the ARRIVE guidelines, Br. J. Pharmacol. 160 (2010) 1577–1579, https://doi.org/10.1111/j.1476-5381.2010.00872.x.
[33] B.F. Cravatt, K. Demarest, M.P. Patricelli, M.H. Bracey, D.K. Giang, B.R. Martin, A.H. Lichtman, Supersensitivity to anandamide and enhanced endogenous cannabinoid signaling in mice lacking fatty acid amide hydrolase, Proc. Natl. Acad. Sci. U. S. A. 98 (2001) 9371–9376, https://doi.org/10.1073/pnas.161191698.
[34] P.M. Zygmunt, J. Petersson, D.A. Andersson, H. Chuang, M. Sørgård, V. Di Marzo, D. Julius, E.D. Högestätt, Vanilloid receptors on sensory nerves mediate the vasodilator action of anandamide, Nature 400 (1999) 452–457, https://doi.org/10.1038/22761.
[35] A. Eskilsson, T. Matsuwaki, K. Shionoya, E. Mirrasekhian, J. Zajdel, M. Schwaninger, D. Engblom, A. Blomqvist, Immune-induced fever is dependent on local but not generalized prostaglandin E, J. Neurosci. 37 (2017) 5035–5044, https://doi.org/10.1523/JNEUROSCI.3846-16.2017.
[36] L. Engström Ruud, D.B. Wilhelms, A. Eskilsson, A.M. Vasilache, L. Elander, D. Engblom, A. Blomqvist, Acetaminophen reduces lipopolysaccharide-induced fever by inhibiting cyclooxygenase-2, Neuropharmacology 71 (2013) 124–129, https://doi.org/10.1016/j.neuropharm.2013.03.012.
[37] E. Mirrasekhian, J.L.Å. Nilsson, K. Shionoya, A. Blomgren, P.M. Zygmunt, D. Engblom, E.D. Högestätt, A. Blomqvist, The antipyretic effect of paracetamol occurs independent of transient receptor potential ankyrin 1-mediated hypothermia and is associated with prostaglandin inhibition in the brain, Faseb. J. 32 (2018) 5751–5759, https://doi.org/10.1096/fj.201800272R.
[38] A.S. Rice, D. Cimino-Brown, J.C. Eisenach, V.K. Kontinen, M.L. Lacroix-Fralish, I. Machin, J.S. Mogil, T. Stöhr, P.P. Consortium, Animal models and the prediction of efficacy in clinical trials of analgesic drugs: a critical appraisal and call for uniform reporting standards, Pain 139 (2008) 243–247, https://doi.org/10.1016/j.pain.2008.08.017.
[39] J.C. Mossanen, F. Tacke, Acetaminophen-induced acute liver injury in mice, Lab. Anim. 49 (2015) 30–36, https://doi.org/10.1177/0023677215570992.
[40] P.M. Zygmunt, E.D. Hogestatt, TRPA1, Handbook of experimental pharmacology 222 (2014) 583–630, https://doi.org/10.1007/978-3-642-54215-2_23.
[41] I. Tubert-Brohman, O. Acevedo, W.L. Jorgensen, Elucidation of hydrolysis mechanisms for fatty acid amide hydrolase and its Lys142Ala variant via QM/MM simulations, J. Am. Chem. Soc. 128 (2006) 16904–16913, https://doi.org/10.1021/ja065863s.
[42] F. Yang, X. Xiao, W. Cheng, W. Yang, P. Yu, Z. Song, V. Yarov-Yarovoy, J. Zheng, Structural mechanism underlying capsaicin binding and activation of the TRPV1 ion channel, Nat. Chem. Biol. 11 (2015) 518–524, https://doi.org/10.1038/nchembio.1835.
[43] E. Cao, M. Liao, Y. Cheng, D. Julius, TRPV1 structures in distinct conformations reveal activation mechanisms, Nature 504 (2013) 113–118, https://doi.org/10.1038/nature12823.
[44] Y. Wang, W. Lin, N. Wu, X. He, J. Wang, Z. Feng, X.Q. Xie, An insight into paracetamol and its metabolites using molecular docking and molecular dynamics simulation, J. Mol. Model. 24 (2018) 243, https://doi.org/10.1007/s00894-018-3790-9.
[45] S. Boukalova, L. Marsakova, J. Teisinger, V. Vlachova, Conserved residues within the putative S4-S5 region serve distinct functions among thermosensitive vanilloid transient receptor potential (TRPV) channels, J. Biol. Chem. 285 (2010) 41455–41462, https://doi.org/10.1074/jbc.M110.145466.
[46] E. Palovcak, L. Delemotte, M.L. Klein, V. Carnevale, Comparative sequence analysis suggests a conserved gating mechanism for TRP channels, J. Gen. Physiol. 146 (2015) 37–50, https://doi.org/10.1085/jgp.201411329.
[47] K. Ohbuchi, Y. Mori, K. Ogawa, E. Warabi, M. Yamamoto, T. Hirokawa, Detailed analysis of the binding mode of vanilloids to transient receptor potential vanilloid type I (TRPV1) by a mutational and computational study, PLoS One 11 (2016), e0162543, https://doi.org/10.1371/journal.pone.0162543.
[48] S. Hunskaar, K. Hole, The formalin test in mice: dissociation between inflammatory and non-inflammatory pain, Pain 30 (1987) 103–114.
[49] G.W. Przybyla, K.A. Szychowski, J. Gminski, Paracetamol - an old drug with new mechanisms of action, Clin. Exp. Pharmacol. Physiol. (2020), https://doi.org/10.1111/1440-1681.13392.
[50] C. Sinning, B. Watzer, O. Coste, R.M. Nüsing, I. Ott, A. Ligresti, V. Di Marzo, P. Imming, New analgesics synthetically derived from the paracetamol metabolite N-(4-hydroxyphenyl)-(5Z,8Z,11Z,14Z)-icosatetra-5,8,11,14-enamide, J. Med. Chem. 51 (2008) 7800–7805, https://doi.org/10.1021/jm800807k.
[51] A. Blomqvist, D. Engblom, Neural mechanisms of inflammation-induced fever, Neuroscientist 24 (2018) 381–399, https://doi.org/10.1177/1073858418760481.
[52] M.J. Eberhardt, F. Schillers, E.M. Eberhardt, L. Risser, J. de la Roche, C. Herzog, F. Echtermeyer, A. Leffler, Reactive metabolites of acetaminophen activate and sensitize the capsaicin receptor TRPV1, Sci. Rep. 7 (2017) 12775, https://doi.org/10.1038/s41598-017-13054-3.
[53] F. Echtermeyer, M. Eberhardt, L. Risser, C. Herzog, F. Gueler, M. Khalil, M. Engel, F. Vondran, A. Leffler, Acetaminophen-induced liver injury is mediated by the ion channel TRPV4, Faseb. J. 33 (2019) 10257–10268, https://doi.org/10.1096/fj.201802233R.
[54] H. Song, T.S. Chen, p-Aminophenol-induced liver toxicity: tentative evidence of a role for acetaminophen, J. Biochem. Mol. Toxicol. 15 (2001) 34–40.
[55] J.L.Å. Nilsson, A. Blomgren, U.J. Nilsson, E.D. Högestätt, L. Grundemar, N,N'-Bis(2-mercaptoethyl)isophthalamide binds electrophilic paracetamol metabolites and prevents paracetamol-induced liver toxicity, Basic Clin. Pharmacol. Toxicol. (2018), https://doi.org/10.1111/bcpt.13058.
[56] M.H. Bracey, M.A. Hanson, K.R. Masuda, R.C. Stevens, B.F. Cravatt, Structural adaptations in a membrane enzyme that terminates endocannabinoid signaling, Science 298 (2002) 1793–1796, https://doi.org/10.1126/science.1076535.